PHYSICAL REVIEW B VOLUME 58, NUMBER 12 15 SEPTEMBER 1998-II

Coherent phonons from the CDW state in η-Mo_4O_{11}

Kisoda Kenji,* Muneaki Hase, Hiroshi Harima, and Shin-ichi Nakashima
Department of Applied Physics, Osaka University, 2-1 Yamadaoka, Suita, Osaka, 565-0871, Japan

Masahiko Tani and Kiyomi Sakai
Kansai Advanced Research Center, Ministry of Posts and Telecommunications, Iwaoka, Nishi-ku, Kobe, 651-2401, Japan

Hiroshi Negishi and Masasi Inoue
Graduate School of Advanced Sciences of Matter, Hiroshima University, Kagamiyama 1-3-1, Higashi Hiroshima, 739-8526, Japan

(Received 15 May 1998)

The charge-density-wave (CDW) phase transition in η-Mo_4O_{11} is studied by femtosecond time-resolved reflection. We observed coherent optical phonons in the reflectivity signal in both the normal and the CDW states. Below the transition temperature T_{c1}, six vibrational modes were clearly detected. Four of them, centered at 64, 78, 85, and 98 cm^{-1}, were enhanced below T_{c1}. We conclude that the generation of these coherent phonon modes are closely related to the CDW state. [S0163-1829(98)50140-3]

I. INTRODUCTION

By virtue of the recent development of femtosecond lasers, femtosecond time-domain spectroscopies, especially using pump-probe techniques, have been applied to studies of coherent phonons in various materials.[1–6] Impulsively and coherently excited optical phonons are called coherent phonons. The term ''coherent'' reminds us of the coherent states used frequently in quantum optics.[7] Coherent phonons partially possess the properties of coherent states. An analogy between the phonons and photons has been discussed recently in terms of quantum optics view point.[8,9]

Time-domain spectroscopies, as well as frequency-domain spectroscopies,[11] have been used to study phase transitions in condensed matters. Among these transitions are superconducting ones[4] in addition to metal-insulator,[1] and structural[10] ones. On the other hand, to the best of our knowledge, no study on charge-density-wave (CDW) phase transitions by time-domain spectroscopy has been reported.

To study CDW phase transitions by time-domain spectroscopy, we chose a quasi-two-dimensional conductor η-Mo_4O_{11} as a CDW sample. The Magnèli phase Mo_4O_{11} has two modifications, monoclinic η- and orthorhombic η-Mo_4O_{11}, both being quasi-two-dimensional metals at room temperature. The η-Mo_4O_{11} undergoes two CDW phase transitions at $T_{c1}=105$ K and $T_{c2}=35$ K.[12–14,19] The existence of CDW in η-Mo_4O_{11} has been established by various measurements such as electrical resistivity and electron diffraction.[13,12–14]

Spectroscopic studies on η-Mo_4O_{11} are relatively few. Guyot *et al.* reported that the IR reflectivity at 15 K decreased compared to that at 300 K although the spectral profiles were similar to each other.[15] They ascribed this decrease in the IR reflectivity to the loss of carriers induced by the CDW gap opening. In addition, no significant change in the Raman spectra was detected around the transition temperatures except for an A_g mode at 98 cm^{-1}; this mode was detected only below T_{c1}.

We carried out the femtosecond pump-probe experiments on the reflectivity of a quasi-two-dimensional conductor η-Mo_4O_{11} at various temperatures. The time-domain result was compared with Raman spectra by the use of a Fourier transform. Coherent phonons have been observed in both the CDW and the normal states. The amplitudes of coherent phonons with frequencies below 100 cm^{-1} show drastic enhancements as the temperature decreases below T_{c1}. By considering temperature dependence of these coherent phonons, we conclude that the generation mechanism of coherent phonons is closely related to the lattice distortion due to the CDW phase transition.

II. EXPERIMENT

Single crystals of η-Mo_4O_{11} were grown by chemical vapor transport using $TeCl_4$ as a transport agent. The source materials (MoO_2 and MoO_3) at the appropriate molar ratio (1:3) and the transport agent were sealed in an evacuated quartz tube and heated at 560−510 °C in a two-zone furnace. The CDW phase transition was identified by measuring electrical resistivity. The η-Mo_4O_{11} crystal belongs to the C_{2h}^5 ($P2_1/a$) space group above T_{c1}.[16] From the factor group analysis, the vibrational modes at the Γ point are decomposed into the following representations for the C_{2h} symmetry:

$$\Gamma = 45A_g + 45B_g + 45A_u + 45B_u .$$

The sample was excited by pulses from a mode-locked Ti:sapphire laser with a wavelength of about 8000 Å with a 50-mW average power. The pulse duration was about 80 fs, and the repetition rate was 82 MHz. The pump and probe pulses were focused on the bc plane of the sample. The probe beam was polarized perpendicular to the pump beam. The pump beam was modulated at the rate of 620 Hz with a shaker and the detected signal is thus a time derivative of reflectivity change $(\partial/\partial t)(\Delta R/R_0)$. Fractional changes ΔR were of the order of 10^{-6}. To analyze the time-resolved signals and compare them with Raman spectra, we used fast

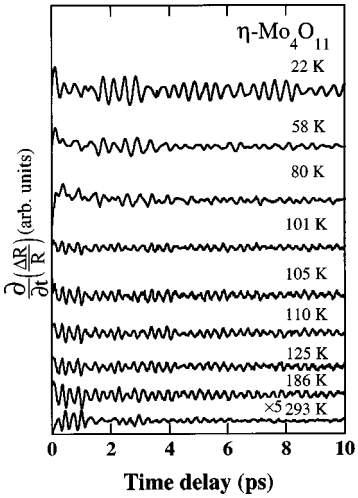

FIG. 1. The time derivatives of the reflectivity change plotted as a function of time delay measured at various temperatures.

Fourier transform. For the temperature measurement, the samples were mounted on the cold finger of a cryostat. Raman-scattering measurement was performed in the quasi-back scattering geometry by using 50-mW cw Ti:sapphire laser also tuned to $\lambda = 8000$ Å.

III. RESULTS AND DISCUSSION

The derivatives of the reflectivity change $\Delta R/R_0$ at various temperatures are plotted as a function of time delay in Fig. 1. Oscillatory features are clearly seen below room temperature. Beating is seen in traces at low temperature while no clear beating is observed above the first transition temperature T_{c1} (105 K). The beating indicates that there are multiple oscillations at low temperature.

Fourier transform (FT) spectra are presented in Fig. 2. There are six phonon peaks, at peak frequencies of about 64, 73, 78, 85, 98, and 121 cm^{-1}, in each FT spectrum below T_{c1}. All bands in the FT spectra, except the 64 cm^{-1} band, correspond to the A_g symmetry Raman bands. On cooling the sample from T_{c1} down to 22 K, the phonon frequencies upshift by 1 to 3 cm^{-1}. As also seen in Fig. 2, the bands at

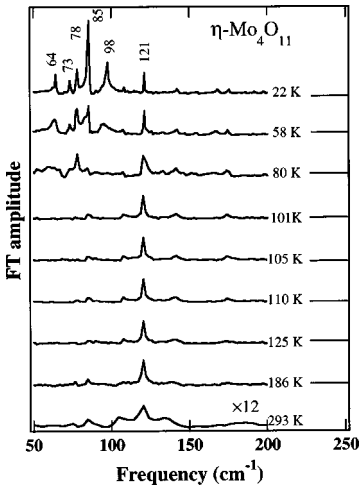

FIG. 2. FT spectra of the time domain in Fig. 1 shown for various temperatures.

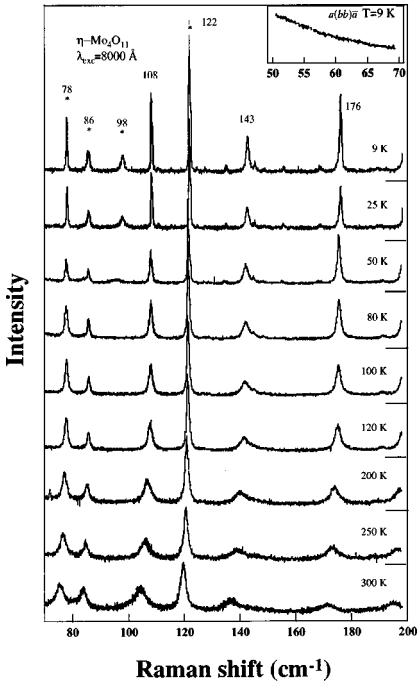

FIG. 3. Unpolarized Raman spectra of η-Mo_4O_{11} taken with 8000-Å excitation at various temperatures. Inset: polarized Raman spectrum in the frequency range 50–70 cm^{-1} at 9 K.

64, 78, 85, and 98 cm^{-1} exhibit strong temperature dependence. The amplitude of these four bands increases suddenly with decreasing temperature. And they almost disappear in the normal state. It is expected that phonon vanishing occurs at the first transition temperature. Nevertheless, the temperature at which the phonons vanish is slightly lower than T_{c1}. Heating effect by the laser brings about the lowering of the temperature at which the phonons are expected to disappear. Above T_{c1}, only one mode (at 120 cm^{-1}) is seen.

Figure 3 shows unpolarized Raman spectra of η-Mo_4O_{11} in a low-frequency range at various temperatures. We observe a number of phonon bands among which the bands at 78, 86, 98, and 122 cm^{-1} are also observed in the pump-probe measurement. All the bands except the band at 98 cm^{-1} are seen below and above T_{c1}. Polarization Raman measurements (not presented here) indicate that these bands are the fully symmetric A_g modes. In the temperature range studied here, the width of each Raman band is slightly wider than that of the corresponding coherent phonon. The 98-cm^{-1} Raman band, as well as the corresponding coherent phonon band, is observed only below T_{c1}. The intensity and frequency of the two Raman bands at 78 and 86 cm^{-1} show no discontinuous change at around T_{c1}. In addition, we did not observe any significant change in the phonon Raman spectra at the second CDW transition temperature T_{c2}.

As shown in the inset of Fig. 3, no phonon band was observed at around 64 cm^{-1} in the polarized Raman spectrum at 9 K taken with the $a(bb)\bar{a}$ geometry. We did not observe any Raman band around 64 cm^{-1} above T_{c1} either. This result suggests that the coherent phonon at 64 cm^{-1} is a Raman inactive mode.

The amplitudes of FT bands at 64, 78, 85, and 98 cm^{-1} normalized to that of a band at 120 cm^{-1} are plotted against temperature in Fig. 4(a). We chose the 120 cm^{-1} band as a

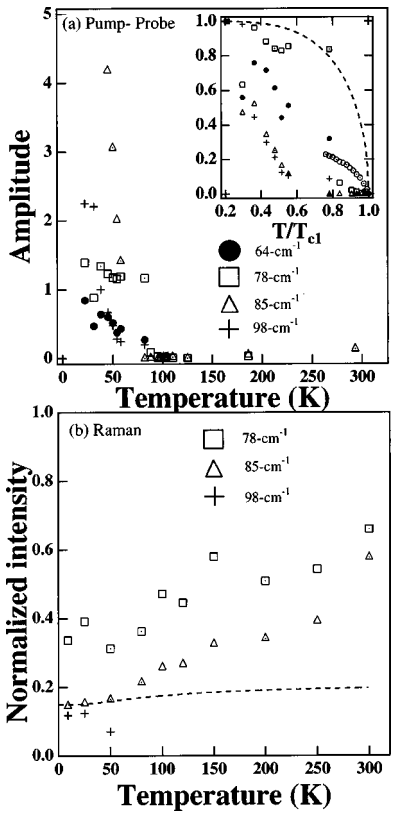

FIG. 4. (a) Temperature dependence of the peak amplitudes of 64, 78, 85, and 98 cm^{-1} bands. Each intensity is normalized to the amplitude of the 120-cm^{-1} mode. Inset: the amplitudes versus a reduced temperature T/T_{c1}. The broken curve shows the temperature dependence of the gap parameter in terms of the weak-coupling BCS theory and the open circle shows the estimated gap from the transport data. The amplitudes are normalized by those at 22 K in the inset. (b) Temperature dependence of the integrated intensities of the Raman bands at 78, 85, and 98 cm^{-1} normalized to that of the 120-cm^{-1} band.

reference because (i) it was present in both normal and CDW states, (ii) the peak amplitude did not show significant temperature dependence, and (iii) the absolute oscillation amplitude was difficult to be evaluated at various temperatures. Figure 4(a) shows that below T_{c1} the FT amplitudes of 64, 78, 85, and 98 cm^{-1} phonons are enhanced drastically on cooling and that these bands almost disappear above T_{c1}. This disappearance is not due to the damping because the widths of these bands remain finite even at around T_{c1}. For example, the width (FWHM) of the 85-cm^{-1} coherent phonon band increases slightly from 2 cm^{-1} (22 K) to 4 cm^{-1} (82 K). The enhancement of the amplitude below T_{c1} suggests that the generation of these four coherent phonons is closely related to the lattice distortion that accompanies the CDW phase transition. Within the framework of a weak coupling BCS-like theory for CDW's, the atomic displacement is given in terms of the gap parameter $\Delta(T)$ and other parameters such as the electron-phonon coupling constant.[17] According to the relation between the displacement and $\Delta(T)$,[17] the displacement shows a temperature dependence similar to that of the gap parameter: the displacement increases with decreasing temperature in the CDW state and becomes zero above T_{c1}.

The amplitudes normalized to those at 22 K are shown in the inset of Fig. 4(a). The horizontal axis is the reduced temperature T/T_{c1}. The broken line represents the temperature dependence of the gap parameter derived from the weak-coupling BCS model and the open circles represent that estimated from transport data.[19] The theoretical and the experimental gaps are normalized to respective $\Delta(0)$'s. As shown in the inset, the amplitudes exhibit a sharper decrease with increasing temperature than those of the gap parameters and become zero at a temperature slightly lower than T_{c1}. The deviation from the calculated curve for the gap is not surprising because the model is mainly used in quasi-one-dimensional CDW conductors. The FT amplitude for the CDW state might be used as the order parameter of the CDW transition even though the temperature dependence of the amplitude is different from that of the actual gap. Further studies on the temperature dependence of the FT amplitudes is required. We also note that the amplitudes exhibit a dip around T_{c2} in the inset. At present, it is unclear whether this dip comes from the second CDW transition at T_{c2}.

Integrated intensities of Raman bands (78,85, and 98 cm^{-1}) normalized to that of the 120-cm^{-1} band are plotted against temperature in Fig. 4(b). Comparing Fig. 4(a) with Fig. 4(b), it is clear that the Raman bands at 78 and 85 cm^{-1} and the corresponding FT bands show completely different temperature dependence. That is, the integrated intensities of these Raman bands increase almost linearly with temperature, whereas the amplitudes of corresponding FT bands show a drastic change at around T_{c1}. The 98-cm^{-1} Raman band and the corresponding coherent phonon amplitude show a similar temperature dependence; that is, both the integrated intensity and the FT amplitude decrease with increasing temperature and disappear above 90 K.

The understanding of the generation mechanism for coherent phonons is still an unsettled issue, especially for opaque materials. Various mechanisms have been proposed; *displacive excitations* of coherent phonons (DECP) in semimetals,[1] ultrafast screening of the surface space charge field in GaAs,[2] and transient stimulated Raman scattering (TSRS) in transparent materials.[6,18] The temperature dependence of coherent phonon amplitudes is different for different modes as shown in Figs. 2 and 4(a) and an additional coherent phonon (Raman inactive) is generated. The anomalous temperature dependence of the coherent phonons below T_{c1} can be explained in terms of DECP: below T_{c1}, the CDW gap in the electronic band is formed and the lattice is distorted simultaneously. High-density excitation of quasiparticles by pump pulses will induce the abrupt destruction of the CDW state and then the gap will close. As a result, the free energy of the lattice subsystem will remain higher than that of the normal state. As a result of this abrupt change in the electronic state, the lattice deformation becomes unstable and the atoms in the crystal will be displaced from the distorted position towards the equilibrium position of the normal state. In this way, the lattice will start to oscillate after the arrival of pump pulses. A similar generation mechanism has been proposed in the superconducting state of YBCO.[20] Mazin *et al.* claimed that the abrupt breakup of the Cooper pair by pump pulses changes the ion positions toward the equilibrium position of the normal state and this process in-

duces the coherent oscillation in the superconducting state of YBCO.

Guyot *et al.* pointed out that the physical properties of η-Mo_4O_{11} are similar to those of the transition-metal dichalcogenides.[14] The displacements of atoms accompanied by the CDW are not necessary equivalent in η-Mo_4O_{11} which is built with infinite slabs of MoO_6 octahedra separated by layers of MoO_4 tetrahedra.[16] The structure of MoO_4 tetrahedra and MoO_6 octahedra would remain unchanged below T_{c1} and relative displacement of MoO_6 octahedra, for example, might induce the Peierls distortion. As a matter of fact, the nesting wave vectors are estimated as $\vec{q_1}=(0,0.23b^*,0)$ and $\vec{q_2}=(?,0.42b^*,0.28c^*)$ below T_{c1} and T_{c2}, respectively.[21] This suggests that the magnitude and the direction of the distortion below T_{c1} differ from those below T_{c2}. When the lattice deformation relevant to a given phonon mode is large, the amplitude of the coherent phonon amplitude is expected to be large. On the other hand, the coherent phonon amplitude would be very small for higher frequency modes which are not influenced much by the CDW transition.

In the normal state of η-Mo_4O_{11}, only one A_g mode at 120 cm^{-1} was detected by the pump-probe measurement. We discarded the other modes (at $\approx$80 and 110 cm^{-1}) because these bands were not reproducible in pump-probe measurements above T_{c1}. The η-Mo_4O_{11} is a metal in the normal state. Since the carrier density is quite high (almost 10^{22} cm^{-3}),[15,19] the carrier density excited by laser pulses is negligibly small compared to the background carrier density. This reduces the efficiency of the generation of coherent phonons above T_{c1}. Comparison of the FT spectra with the Raman spectra demonstrates that there is no correlation between time-domain and Raman-scattering intensities in the normal state. The TSRS model[6] is probably inapplicable to the coherent phonon generation.[6] The coherent phonon generation via ultrafast screening of a surface charge field can also be excluded because η-Mo_4O_{11} is metallic in the normal state and because the surface space-charge field does not exist.

In summary, we have observed coherent phonon oscillations from both the CDW and the normal states of η-Mo_4O_{11}. In the CDW state, six coherent phonon modes were excited. Moreover, below T_{c1}, the amplitudes of four of these coherent phonons (at 64, 78, 85, and 98 cm^{-1}) are drastically enhanced with decreasing temperature. We conclude from the present result that the generation of coherent phonons is correlated strongly with the Peierls distortion.

ACKNOWLEDGMENTS

Dr. Kohji Mizoguchi is much appreciated for helping with the early stage of the time-domain experiment. One of the authors (K.K.) thanks Dr. Oleg V. Misochko for carefully reading the manuscript and giving useful comments.

*Electronic address: kisoda@ap.eng.osaka-u.ac.jp

[1] H. J. Zeiger, J. Vidal, T. K. Cheng, E. P. Ippen, G. D. Dresselhaus, and M. S. Dresselhaus, Phys. Rev. B **45**, 768 (1992); H. J. Zeiger, T. K. Cheng, E. P. Ippen, J. Vidal, G. D. Dresselhaus, and M. S. Dresselhaus, *ibid.* **54**, 105 (1996).

[2] G. C. Cho, W. Kütt, and H. Kurz, Phys. Rev. Lett. **65**, 764 (1990).

[3] T. Pfeifer, R. Scholz, and H. Kurz, Phys. Rev. Lett. **69**, 3248 (1992).

[4] W. Albrecht, Th. Kruse, and H. Kurz, Phys. Rev. Lett. **69**, 1451 (1992).

[5] W. Kütt, W. Albrecht, and H. Kurz, IEEE J. Quantum Electron. **28**, 2434 (1992); L. Dhar, J. A. Rogers, and K. A. Nelson, Chem. Rev. **94**, 157 (1994).

[6] G. A. Garrett, T. F. Albrecht, J. F. Whitaker, and R. Merlin, Phys. Rev. Lett. **77**, 3661 (1996).

[7] See for example, John R. Klauder and Bo-Sture Skagerstam, *Coherent States: Applications in Physics and Mathematical Physics* (World Scientific, Singapore, 1985), and references therein.

[8] X. Hu and F. Nori, Phys. Rev. Lett. **76**, 2294 (1996); **79**, 4605 (1997).

[9] G. A. Garrett, J. F. Whitaker, A. K. Sood, and R. Merlin, Science **275**, 1638 (1997).

[10] T. P. Dougherty, G. P. Wiederrecht, K. A. Nelson, M. H. Garrett, H. P. Jensen, and C. Warde, Science **258**, 770 (1992).

[11] S. Sugai, Phys. Status Solidi B **127**, 2 (1984).

[12] For a recent review, see C. Schlenker, J. Dumas, C. Escribe-Filippini, and H. Guyot, in *Low-Dimensional Electronic Properties of Molybdenum Bronzes and Oxides*, edited by C. Schlenker (Kluwer, the Netherlands, 1989).

[13] H. Guyot, C. Escribe-Filippini, G. Fourcaudot, K. Konate, and C. Schlenker, J. Phys. C: Solid State Phys. **16**, L1227 (1983).

[14] H. Guyot, C. Schlenker, J. P. Pouget, R. Ayroles, and C. Roucau, J. Phys. C: Solid State Phys. **18**, 4427 (1985).

[15] H. Guyot, E. Al Khoury, J. Marcus, C. Schlenker, M. Banville, and S. Jandl, Solid State Commun. **79**, 307 (1991).

[16] L. Kihlborg, Ark. Kemi **21**, 365 (1963).

[17] G. Grüner, *Density Waves in Solids* (Addison-Wesley, Reading, 1994).

[18] R. Merlin, Solid State Commun. **102**, 207 (1997).

[19] S. Ohara, M. Koyano, H. Negishi, M. Sasaki, and M. Inoue, Phys. Status Solidi B **164**, 243 (1991); M. Sasaki, G. X. Tai, M. Koyano, and M. Inoue, Phys. Rev. B **47**, 6216 (1993); M. Sasaki, G. Houzaki, M. Koyano, and M. Inoue, J. Phys. Chem. Solids **57**, 281 (1995); M. Inoue, S. Ohara, S. Horisaka, M. Koyano, and H. Negishi, Phys. Status Solidi B **148**, 659 (1988).

[20] I. I. Mazin, A. I. Liechtenstein, O. Jepsen, O. K. Andersen, and C. O. Rodriguez, Phys. Rev. B **49**, 9210 (1994); S. J. Nettle and R. K. MacCrone, *ibid.* **49**, 6395 (1994).

[21] P. Foury and J. P. Pouget, Int. J. Mod. Phys. B **7**, 3973 (1993).